Developmental Biology 448 (2019) 173–182

Contents lists available at ScienceDirect

Developmental Biology

journal homepage: www.elsevier.com/locate/developmentalbiology

Original research article

Wavy movements of epidermis monocilia drive the neurula rotation that determines left–right asymmetry in ascidian embryos

Shiori Yamada[1], Yuka Tanaka[1], Kaoru S. Imai, Motohiko Saigou, Takeshi A. Onuma, Hiroki Nishida*

Department of Biological Sciences, Graduate School of Science, Osaka University, 1-1 Machikaneyama-cho, Toyonaka, Osaka 560-0043, Japan

ARTICLE INFO

Keywords:
Left–right asymmetry
Cilia
Neurula rotation
Nodal
Ascidian
Halocynthia roretzi

ABSTRACT

Tadpole larvae of the ascidian, *Halocynthia roretzi*, show morphological left–right asymmetry in the brain structures and the orientation of tail bending within the vitelline membrane. Neurula embryos rotate along the anterior–posterior axis in a counterclockwise direction, and then this rotation stops when the left side of the embryo is oriented downwards. Contact of the left-side epidermis with the vitelline membrane promotes *nodal* gene expression in the left-side epidermis. This is a novel mechanism in which rotation of whole embryos provides the initial cue for breaking left–right symmetry. Here we show that epidermal monocilia, which appear at the neurula rotation stage, generate the driving force for rotation. A ciliary protein, Arl13b, fused with Venus YFP was used for live imaging of ciliary movements. Although overexpression of wild-type Arl13b fusion protein resulted in aberrant movements of the cilia and abrogation of neurula rotation, mutant Arl13b fusion protein, in which the GTPase and coiled-coil domains were removed, did not affect the normal ciliary movements and neurula rotation. Epidermis cilia moved in a wavy and serpentine way like sperm flagella but not in a rotational way or beating way with effective stroke and recovery stroke. They moved very slowly, at 1/7 Hz, consistent with the low angular velocity of neurula rotation (ca. 43°/min). The tips of most cilia pointed in the opposite direction of embryonic rotation. Similar motility was also observed in *Ciona robusta* embryos. When embryos were treated with a dynein inhibitor, Ciliobrevin D, both ciliary movements and neurula rotation were abrogated, showing that ciliary movements drive neurula rotation in *Halocynthia*. The drug also inhibited *Ciona* neurula rotation. Our observations suggest that the driving force of rotation is generated using the vitelline membrane as a substrate but not by making a water current around the embryo. It is of evolutionary interest that ascidians use ciliary movements to break embryonic left–right symmetry, like in many vertebrates. Meanwhile, ascidian embryos rotate as a whole, similar to embryos of non-vertebrate deuterostomes, such as echinoderm, hemichordate, and amphioxus, while swimming.

1. Introduction

Various types of animals show a stereotyped left–right (L-R) asymmetry in their body, both in external and internal organization. Embryos start their development in a symmetrical manner, then at a certain stage, the L-R symmetry is broken by key events (Spéder et al., 2007; Vandenberg and Levin, 2013; Namigai et al., 2014; Blum et al., 2014). In vertebrates, such as mouse, frog and fish, breaking symmetry is carried out using motile cilia within the L-R organizer (Nonaka et al., 1998; Okada et al., 2005). Cilia in the node of mouse rotate 600 rpm and generate leftward nodal flow, and eventually left-side-specific *nodal* gene expression is promoted in lateral plate mesoderm (Nonaka et al., 2002; Takaoka et al., 2007). Ascidians are the closest relatives of vertebrates, and their embryos develop into tadpole larvae with a simple chordate body plan. The tadpole larvae show morphological L-R asymmetry in tail bending within the vitelline membrane and brain structures (Taniguchi and Nishida, 2004; Morokuma et al., 2002). They also express *nodal* and *Pitx2* genes in the left-side epidermis in the neurula to tailbud stages (Morokuma et al., 2002; Yoshida and Saiga, 2008, 2011). It is of interest how ascidians utilize motile cilia for symmetry breaking.

Ascidian embryos do not have a cavity corresponding to the L-R organizer. Instead, the entire embryo rotates along the anterior–posterior axis at the neurula stage (neurula rotation; Fig. 1A) (Nishide et al., 2012). Neurulae of *Halocynthia roretzi* rotate in a counterclockwise direction at 15 h of development; this rotation stops

* Corresponding author.
E-mail address: hnishida@bio.sci.osaka-u.ac.jp (H. Nishida).
[1] These authors equally contributed to this work.

https://doi.org/10.1016/j.ydbio.2018.07.023
Received 26 March 2018; Received in revised form 19 June 2018; Accepted 26 July 2018
Available online 27 July 2018

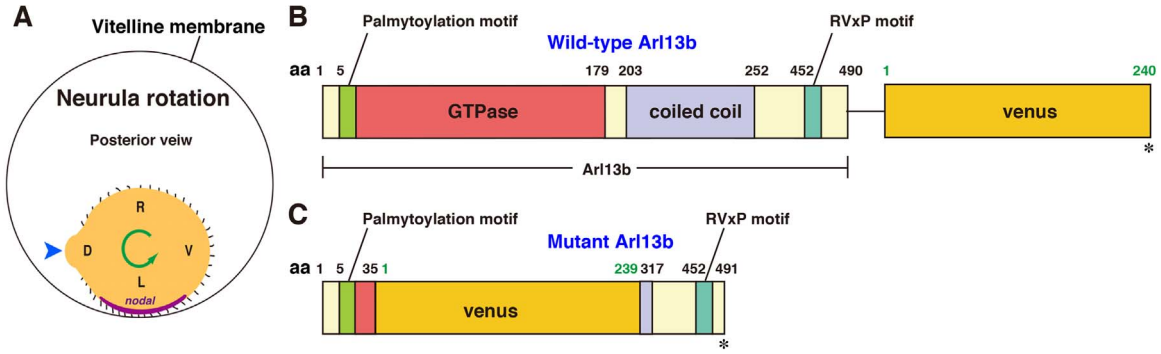

Fig. 1. Neurula rotation and Arl13b fusion proteins. (A) Schematic drawing of neurula rotation. The neurula is viewed from the posterior pole. Neurulae rotate in a counterclockwise direction (arrow) at 15 h of development, and this rotation stops when the left side of the embryo is oriented downwards. Protrusion of the neural fold (arrowhead) physically prevents embryos from rotating further. Contact of epidermis and the vitelline membrane promotes *nodal* expression (purple) in the left-side epidermis. After the completion of neurula rotation, when the embryos are manually rotated 180° so that they lay on their right side, they rotate back 180° and settle on their left side again (re-rotation). This can be repeated many times within 3 h. D, dorsal. L, left. R, right. V, ventral. Modified from Nishide et al. (2012) with permission. (B) Top: Wild-type Arl13b fused to Venus YFP. Bottom: Mutant Arl13b. Central part (aa 36–316) was replaced by Venus YFP. Positions of amino acids of Arl13b are shown in black letters, and those of Venus YFP are in green letters. Asterisks indicate the stop codons.

when the left side of the embryo is oriented downwards. Protrusion of the neural fold (Fig. 1A, arrowhead) physically prevents embryos from rotating further. Contact of the epidermis and vitelline membrane promotes *nodal* expression (Fig. 1A, purple) in the left-side epidermis at 2 h after neurula rotation.

The neurula retain rotation ability for 3 h. After the completion of neurula rotation, when the embryos are manually rotated 180° so that they lay on their right side, they rotate back 180° and settle on their left side again (called re-rotation; Nishide et al., 2012). Observations with scanning electron microscopy and immunohistochemistry with acetylated tubulin have shown that, on the surface of neurula embryos, epidermal cells have monocilia. It has been suggested that those cilia drive neurula rotation because the epidermal cells retain cilia for 3 h, which coincides with the duration of re-rotation ability. However, it is difficult to visualize the movements of cilia in live embryos because the cilia are very short and embryos are opaque. So it has not been known whether cilia are motile and how they move: beating or rotating. Neurula rotation has been observed in five ascidian species so far (Nishide et al., 2012). *Ciona robusta* (formerly *Ciona intestinalis* Type A) also shows neurula rotation and has cilia on the surface (Thompson et al., 2012; Katsumoto et al., 2013; Negishi et al., 2016; Palmquist and Davidson, 2017). However, Thompson et al. (2012) concluded that cilia are not motile in *Ciona* because the axoneme had a nine-doublet microtubule ring structure, but its organization was disorganized in their ultrastructural observation. Brief hypo-osmotic shock resulted in the death of test cells, which are accessory cells of maternal origin within the perivitelline space, and prevented neurula rotation in *Ciona*, suggesting the possible involvement of test cells in neurula rotation (Katsumoto et al., 2013). This suggested that the test cells serve as a 'foothold' for cilia to generate a counter-force of ciliary movement.

Most non-chordate deuterostomes develop embryos and larvae that swim using cilia, such as the blastula and pluteus of sea urchins, the tornaria of hemichordates, and Amphioxus embryos (Satoh, 2009). They rotate in a counterclockwise direction while swimming, which is the same direction of ascidian neurula rotation. By contrast, ascidian larvae swim using their tail. Therefore, it has been proposed as a possible evolutionary scenario across deuterostomes that ascidians might reutilize their ancestral epidermal cilia for neurula rotation but not for swimming (Nishide et al., 2012). It is important to visualize ciliary movements using live imaging to know whether the cilia of ascidians are motile and how they move.

In the present study, we revealed using live imaging that ascidian cilia indeed move to generate a driving force for neurula rotation. We unexpectedly found that ascidian epidermis monocilia move very slowly in a wavy and serpentine way like the flagella of sperm and the single-celled algae, Euglena.

2. Materials and methods

2.1. Embryos

Naturally spawned eggs of the ascidian *Halocynthia roretzi* were fertilized with a suspension of non-self sperm and raised in Millipore-filtered seawater or artificial sea water (Rei-Sea Marine, REI-SEA IWAKI, Tokyo) containing 50 μg/ml streptomycin sulfate and 50 μg/ml kanamycin sulfate at 11–13 °C. Tadpole larvae hatch at 36 h after fertilization at 13 °C.

2.2. Synthetic mRNAs for Arl13b expression

To visualize cilia, Venus YFP was fused to wild-type ADP-ribosylation factor-like protein 13B (Arl13b) or mutant Arl13b (Fig. 1B and C). *H. roretzi* Arl13b homolog (Harore.CG.MTP2014.S25.g08657.01.t; the gene model is not correct, and only 5′ one fifth of the gene model actually corresponds to the Arl13b gene) was identified in *H. roretzi* genome sequences (Aniseed database, https://www.aniseed.cnrs.fr/; Brozovic et al., 2018). An EST clone (ma150c16; GenBank accession No. FY852070.1 and FY886063.1) of the MAGEST *H. roretzi* EST database (http://magest.hgc.jp/; Makabe et al., 2001) contains the entire open reading frame. The orthology was confirmed in the molecular phylogenic tree including Arl13b, Arl13a and Arl1 of various animals. The mRNA is present maternally and gradually decreases but is still present at the larval stage (Aniseed database). To express wild-type fusion protein, the Arl13b ORF of the MAGEST EST clone was fused to the N-terminal of Venus YFP and inserted into the HTB(N) vector that has *H. roretzi* tubulin β UTRs (Akanuma et al., 2002) (Fig. 1B).

To express mutant Arl13b fusion protein, the central part of Arl13b (aa 36–316) was replaced by Venus YFP using an In-Fusion cloning kit (Clonetech Laboratory) and cloned into the HTB(N) vector. This removes most of the GTPase (aa 5–179) and coiled-coil (aa 203–252) domains (Hori et al., 2008) but leaves the palmitoylation motif (aa 8; palmitoylation site) that was identified by CSS-Palm (http://csspalm.biocuckoo.org/) and responsible for transportation to the plasma membrane (Cevik et al., 2010) and the RVxP motif (aa 452–455; KVKP) that was identified by comparison of Arl13b sequences of various animals and is involved in localization to the cilia (Geng et al., 2006) (Fig. 1C). In embryos that expressed mutant Arl13b fusion protein, nuclei and cell membranes were also fluorescently visible (see Fig. 2). Synthetic mRNAs were prepared as described previously (Kumano et al., 2006). mRNA (1.6 and 0.4 μg/μl) was injected into *Halocynthia* eggs after fertilization and *Ciona* eggs before fertilization, respectively.

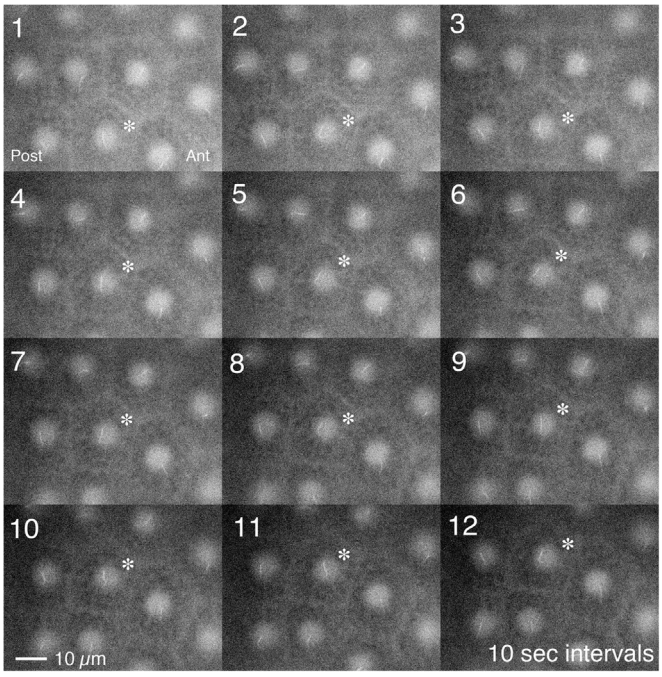

Fig. 2. Serial snapshots of cells and cilia during neurula re-rotation. A neurula embryo was observed from the bottom. Its anterior is to the right. Cilia were visualized using mutant Arl13b fusion protein. The nuclei and cell membrane of epidermal cells are also visible. Serial snapshots were generated using the "Make montage" function of Image J at 10 s intervals. The same cell is marked by asterisks, and this is the cell shown in Fig. 3. Cells are moving upwards. The monocilia are positioned close to the nuclei. Wavy shapes of cilia are recognizable. The serpentine movements are clearly evident in Supplementary Movie S1. Ant, anterior. Post, posterior.

2.3. Microinjection

Vitelline membrane is required for neurula rotation. Devitellinated neurulae do not rotate. Follicle cells on the vitelline membrane were removed by Actinase E (Sigma) treatment after fertilization. Eggs with vitelline membranes were attached onto a coverslip, immobilized and microinjected. Then, eggs with vitelline membranes were gently detached from the coverslip and transferred into gelatin-coated dishes until observation. Deformation of the vitelline membrane perturbed appropriate neurula rotation. We only used embryos with completely a spherical vitelline membrane. Similarly, when injected eggs were left attached on the coverslip, all of them failed to rotate. This is because the bottom of the vitelline membrane was flattened by attachment to the coverslip. It is highly likely that curvature of the vitelline membrane is important and a certain amount of contact between the membrane and embryonic surface is essential to drive rotation. *Ciona* eggs with vitelline membranes, from which follicle cells were removed by gentle pipetting, were held by a suction pipette and injected.

2.4. Microscopy and image analysis

Neurulae start neurula rotation at 15 h after fertilization at 13 °C. They retain rotation ability for 3 h. After the completion of neurula rotation, when the embryos are manually rotated 180° by rotating the vitelline membrane with a tungsten needle so that they lay on their right side, they rotate back 180° and settle on their left side again (called re-rotation; Nishide et al., 2012). This can be repeated many times within 3 h. Therefore, after the completion of neurula rotation, we checked that embryos can re-rotate, and then a right-side-down embryo was transferred into a gelatin-coated glass-bottom dish and the next re-rotation was observed. Embryos that showed fluorescence in the cilia were observed from the bottom with an inverted microscope equipped with Delta Vision (GE Healthcare Life Sciences) and 40× oil-immersion objective (Olympus, U-Apo 40×/1.35 Oil). Time-lapse recording was carried out with 0.1–0.5 s illumination with intervals of 1 or 5 s. Images and movies were processed using Image J. The length of each cilium was measured with the Image J line-tracing function using snapshots from movies.

2.5. Ciliobrevin D treatment

To inhibit ciliary movement, embryos were treated with 30 μM Ciliobrevin D (Merck). Ciliobrevin D inhibits dynein ATPase activity (Firestone et al., 2012). Between 10 and 30 μM, dose-dependency was observed in the inhibition of neurula rotation. It was also confirmed that treatment with 30 μM Ciliobrevin D completely inhibited cell division at the cleavage stage. A stock solution (20 mM in DMSO) was prepared and kept at − 30 °C. The stock solution was diluted with seawater just before use. The solution and embryos were light-shielded to avoid degradation of the drug. After confirmation of the ability of neurula re-rotation of mutant Arl13B-expressing embryos, the embryos were preincubated with Ciliobrevin D for 15 min. Then the next re-rotation and ciliary movement were monitored. Control embryos were treated with DMSO.

2.6. Statics

Data are expressed as the mean ± s.d. The Chi-square test and Student *t*-test were applied to assess significance. Each observation was made in at least three independent experiments unless otherwise stated.

3. Results

3.1. Epidermis monocilia are motile and move very slowly in a serpentine way

Arl13b, an ARF family small GTPase, is a protein transported into cilia (Lu et al., 2015). Cilia of the neurula of *Halocynthia* were visualized by injection of mRNA encoding mutant Arl13b-Venus fusion protein, in which the central part of Arl13b was replaced by Venus but retaining the palmitoylation motif responsible for transportation to plasma membrane and the RVxP motif involved in localization to the cilia (Fig. 1C). Neurula rotation begins at 15 h of development and lasts approximately 10 min over a 90° rotation with angular velocity of approximately 10°/min on average. The length of cilia at this stage was 3.7 μm on average (n = 10). It was not easy to record the processes of neurula rotation because it lasts only 10 min after 15 h of development and because of the natural developmental asynchrony among embryos at this stage.

Therefore, we first monitored ciliary movements during neurula re-rotation. Re-rotation can be repeated several times and is highly reproducible. Neurula re-rotation lasts approximately 5 min for a 180° rotation with an angular velocity of approximately 43°/min. The length of cilia at this stage was 8.0 μm on average (n = 47), but this depends on the time of the observation. Thus, re-rotation is faster than the initial rotation, probably because the cilia are longer and generate a stronger driving force. This coincides with the previous observation of cilia growth over time using a scanning electron microscope (Nishide et al., 2012). There was a tendency that the later re-rotation was monitored, the faster the embryos rotated. Prior to observation of the cilia, we confirmed under a binocular microscope that the embryo was able to re-rotate. Then, the embryos were manually rotated 180° so that they lay on their right side, and they were immediately set for observation of the second re-rotation with a inverted fluorescent microscope. Ciliary movements during re-rotation were recorded from the bottom of the embryos where embryos contact the vitelline membrane. At the neurula stage, test cells are aggregated and they are excluded under the embryos in *Halocynthia*. Therefore, cilia

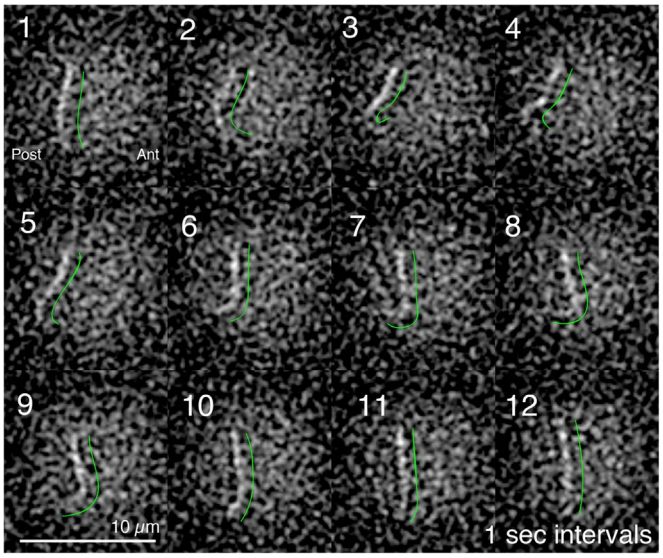

Fig. 3. Serial snapshots of a cilium during a single cycle of wavy movement. A single cell that is marked by asterisks in Fig. 2 was followed using the "StackReg" function (http://bigwww.epfl.ch/thevenaz/stackreg/) of Image J. Snapshots are aligned at 1 s intervals. The shapes of the cilium are traced in green lines. The cilium moved very slowly, at 1/12 Hz, in this case. Ant, anterior. Post, posterior. See also Supplementary Movie S1.

directly contact the vitelline membrane at the bottom.

Monocilia were clearly visualized with mutant Arl13b fusion protein. Nuclei and cell membrane also faintly fluoresced, and this feature was advantageous for monitoring the rotation of the entire embryo. We recorded every 1 s to create time-lapse movies. This was sufficient to monitor the movement of cilia, as they moved very slowly. Each epidermal cell had a monocilium above the nucleus. The base of cilia showed no positional bias, as shown in a previous study (Nishide et al., 2012). Interestingly, the cilia move in a wavy and serpentine way like the flagella of sperm (Figs. 2 and 3; Supplementary Movie S1). This kind of "crawling" movement of cilia on the vitelline membrane was consistently observed many times. To our knowledge, there is no other animal example that monocilia of multicellular epithelium show such a wavy movement. Angular velocities were comparable between uninjected and mutant Arl13b-expressing embryos, suggesting that mutant Arl13b did not affect neurula re-rotation (Fig. 4A; the difference could be accounted for by the difference in stages of observation). A cilium was in a single focal plane along its entire length, suggesting that they lay in the narrow space between embryonic surface and the vitelline membrane. Most of the cilia pointed in the opposite direction to rotation, indicating that cilia generate the driving force of rotation (Fig. 4B). They moved very slowly; a single cycle of ciliary movement was 7.6 s ± 1.5 S.D. with significant variation (Fig. 3, Supplementary Movie S1; note that the movie plays 10 times faster than real time). The slow movement of cilia coincides well with the slow rotation of the entire embryo (approximately 5 min for a 180° rotation). The movements of cilia were not synchronized between them.

To examine whether cilia on the entire surface of embryos move, we observed the cilia on the top of the embryos from above using an upright microscope (Olimpus BX61). In order to observe small cilia, an objective lens of high magnification (100×; oil immersion) was used. Because of the short working distance and wide perivitelline space in *Halocynthia* (Fig. 1A; transverse diameter of the neurula is ca. 200 μm, and that of the perivitelline space is ca. 340 μm), the vitelline membrane, but not embryo, was slightly compressed by the cover slip, causing the bottom and top sides of the membrane to became flattened. This caused the failure of re-rotation in most embryos. It is likely that the curvature of the vitelline membrane at the bottom is important and

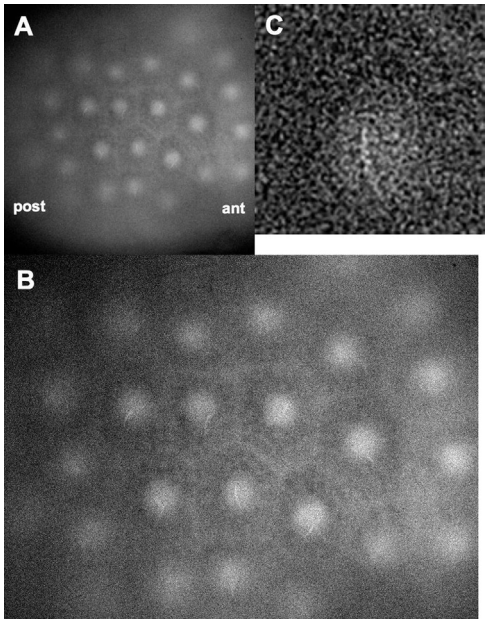

Movie S1. Ciliary movements during neurula re-rotation. Time-lapse recording was carried out with intervals of 1 s. The movie runs at 10 frames/s, so it plays 10 times faster than real time. Note that cilia move very slowly. See also Figs. 2 and 3. (A) Neurula embryo observed from the bottom. Entire view. Anterior is to the right. Cilia were visualized using mutant Arl13b fusion protein. Nuclei and cell membrane of epidermal cells are also visible. The wavy movements of cilia are evident. Ant, anterior. Post, posterior. (B) Closer view. (C) A single cell that is marked by asterisks in Fig. 2 was followed using the "StackReg" function (http://bigwww.epfl.ch/thevenaz/stackreg/) of Image J.Supplementary material related to this article can be found online at doi:10.1016/j.ydbio.2018.07.023.

a certain amount of contact between the membrane and embryonic surface is essential to drive rotation (see also microinjection section of Materials and Methods). Cilia on the top of embryos did not move (Supplementary Movie S2). In contrast, cilia on the bottom under similar conditions did move (data not shown). Many cilia in the movie look like dots or shortened lines because they stood vertically from the embryonic surface, but they are not actually shortened. This was confirmed by gradually changing the focal plane along the length of entire cilium. Therefore, it is highly possible that cilia that do not have contact with the vitelline membrane do not move. It was impossible to observe cilia on the lateral sides because of the large size of *Halocynthia* embryos.

3.2. Overexpression of wild-type Arl13b fusion protein abrogated neurula re-rotation and ciliary movements

We also expressed wild-type Arl13b fused to Venus YFP at the C-terminal (Fig. 1B). The protein was strictly localized to cilia. Neurula

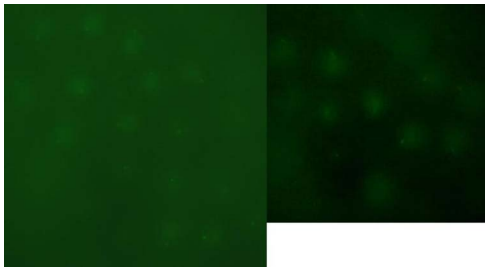

Movie S2. Ciliary movements on the top of embryos Cilia on the top of two embryos were observed from above using an upright microscope. Recordings were carried out with intervals of 0.5 s. The movie runs at 10 frames/s, so it plays five times faster than real time. The cilia are not moving.Supplementary material related to this article can be found online at doi:10.1016/j.ydbio.2018.07.023.

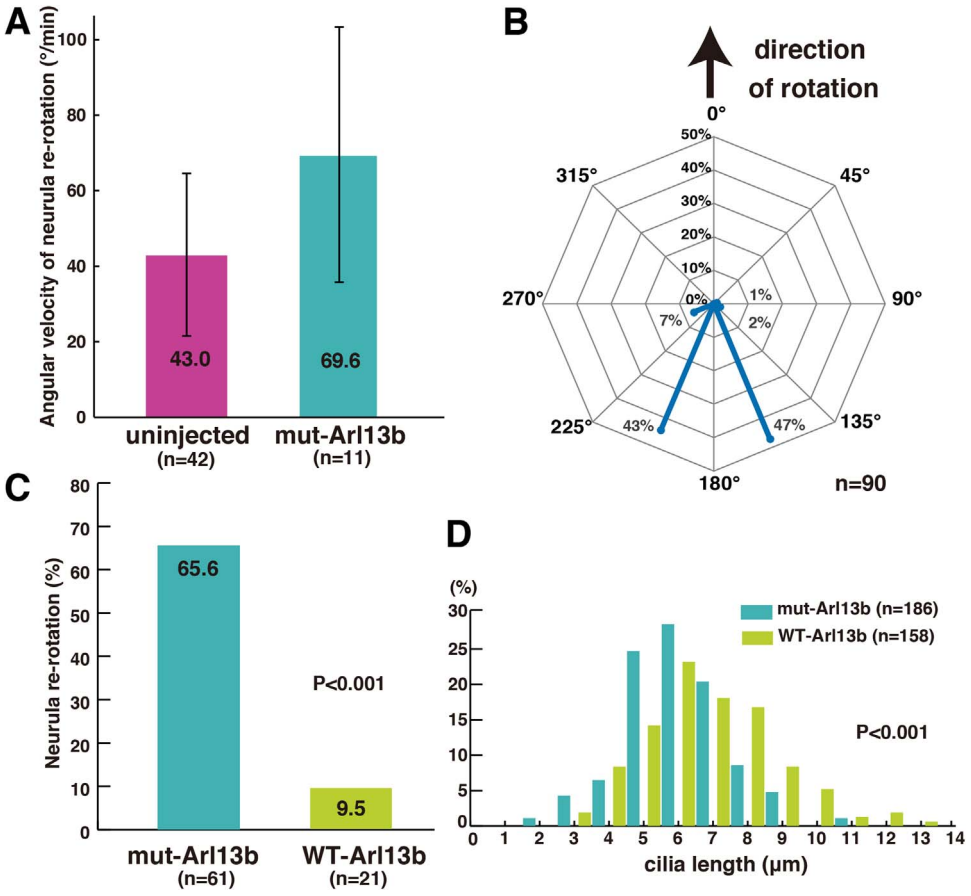

Fig. 4. Various measurements in neurula re-rotation and cilia. (A) Angular velocity of neurula re-rotation. Bars, standard deviation. (B) Angles of cilia referenced with the direction of neurula re-rotation. The direction to which epidermal cells moved in movies is upwards (0°). Angles of 90 cilia were measured in four embryos and counted in each 45° sector. The tips of most cilia pointed in the opposite direction to rotation. (C) Occurrence of neurula re-rotation in wild-type (WT) and mutant (mut) Arl13B fusion protein-expressing embryos. WT-Arl13B suppressed neurula re-rotation. (D) Cilia length in wild-type and mutant Arl13B fusion protein-expressing embryos. Cilia were longer in wild-type expressing embryos.

re-rotation was significantly inhibited by overexpression of wild-type Arl13b (Fig. 4C). Most of the cilia did not move (Fig. 5, arrowheads; Supplementary Movie S3). Some cilia showed weak or unusual motility (Fig. 5, arrows). Sometimes they pointed in the wrong direction. Thus, overexpression of wild-type Arl13b would interfere with the motile function of cilia. Measurement of cilia length at the same neurula stage indicated that cilia expressing wild-type Arl13b (8.5 μm on average) were longer than those expressing mutant Arl13b (6.3 μm) (Fig. 4D). These observations coincide with those reported in mouse culture cells and zebrafish embryos, in which overexpression of wild-type Arl13b results in longer cilia and disturbs their motility (Lu et al., 2015). In the present results, disturbance of cilia motility in ascidian by overexpression of wild-type Arl13b resulted in the failure of neurula re-rotation. Therefore, it is likely that ciliary movements drive neurula rotation.

3.3. Inhibition of dynein motor suppressed neurula re-rotation and ciliary movements

The possibility that ciliary movements drive neurula rotation was further confirmed by inhibition of ciliary movement by a dynein inhibitor, Ciliobrevin D (Firestone et al., 2012). When the treatment was initiated before the neurula rotation stage, cilia formation was inhibited and embryos did not rotate.

We then tried to suppress the movement of cilia that were already formed. After confirmation of the ability for neurula re-rotation in mutant Arl13B-expressing embryos (gray bar in Fig. 6A), the embryos were preincubated with Ciliobrevin D for 15 min. They were manually rotated 180° again, and the occurrence of the next re-rotation and ciliary movement were monitored (Fig. 6A–C and Supplementary Movie S4). Embryos have cilia during this period and do not undergo cell division. Control embryos were treated with DMSO. A total of 94% of embryos re-rotated in the controls. In contrast, none of treated embryos showed re-rotation. Both the control and treated embryos had

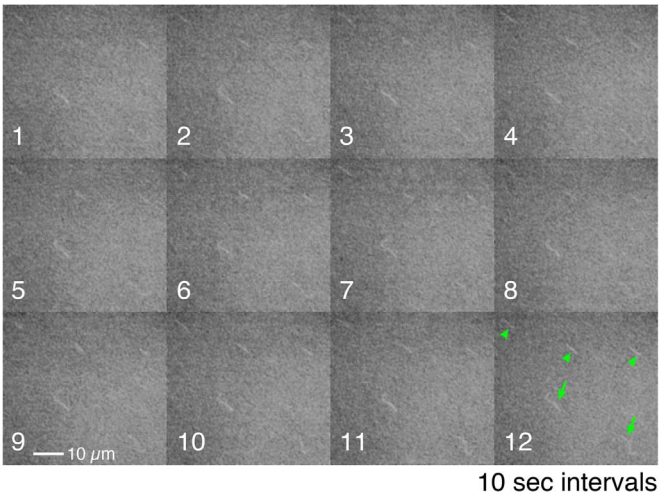

Fig. 5. Ciliary movements in a neurula expressing wild-type Arl13b fusion protein. Snapshots are aligned at 10 s intervals. Five cilia are visible. Three of them do not move (arrowheads). Two are motile, but the movements are lumbering (arrows). The orientations of the cilia are also improper. Two cilia indicated by arrows are oriented in opposite directions to each other. See also Supplementary Movie S3.

Movie S3. Ciliary movements in wild-type Arl13B fusion protein-expressing embryos. Time-lapse recording was carried out with intervals of 1 s. The movie runs at 10 frames/s, so it plays 10 times faster than real time. Some cilia do not move, while the others are motile but their movements are lumbering. See also Fig. 5.Supplementary material related to this article can be found online at doi:10.1016/j.ydbio.2018.07.023.

cilia visualized using mutant Arl13b. In controls, 93% of cilia moved normally, but 80% of treated embryos did not move, and 20% showed irregular and weak movement. Many cilia in the Ciliobrevin D–treated embryos look like dots because they stood vertically, but they were not shortened. This was confirmed by gradually changing the focal plane.

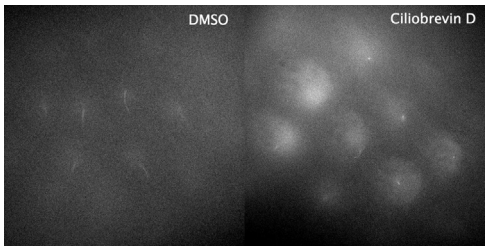

Movie S4. Ciliary movements in embryos treated with the dynein inhibitor, Ciliobrevin D. (Left) Control embryos treated with DMSO. (Right) Embryos treated with Ciliobrevin D. Time-lapse recording was carried out with intervals of 1 s. The movie runs at 10 frames/s, so it plays 10 times faster than real time.Supplementary material related to this article can be found online at doi:10.1016/j.ydbio.2018.07.023.

3.4. Start and stop of neurula rotation and re-rotation

Embryos invariably rotate in a counter-clockwise direction when viewed from the posterior pole. They cease rotation when the left side of the embryo faces down, as the protrusion of the neural fold (Fig. 1A, arrowhead) presents a physical obstacle to further rotation. Cilia are present over the entire surface except in the closing neural fold area (Nishide et al., 2012). First, we observed the behavior of cilia at the end of neurula re-rotation (Fig. 7 and Supplementary Movie S5). When the neural fold came close to the bottom of embryos, rotation stopped. Some cilia in the field of view continued moving, but cilia of epidermal

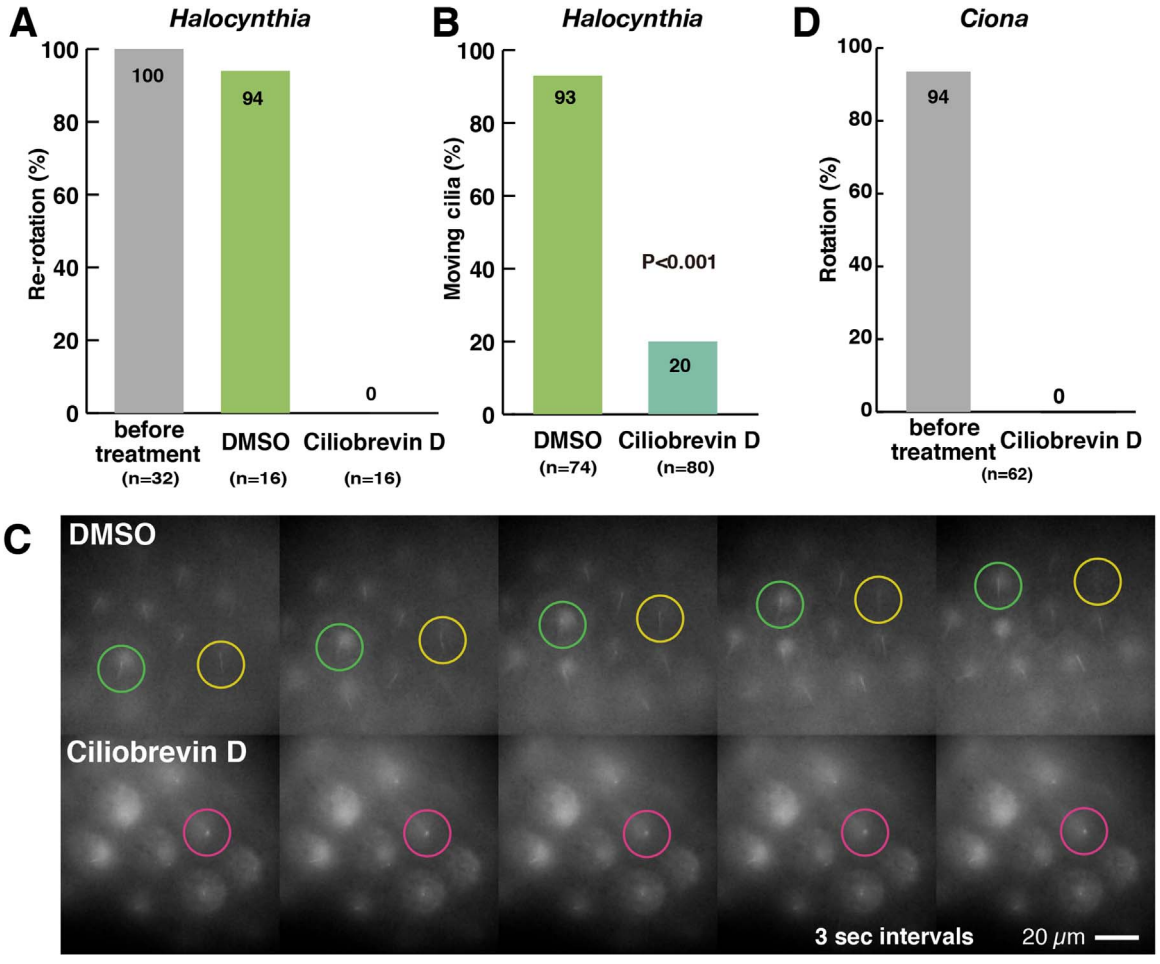

Fig. 6. Dynein inhibitor treatment suppressed neurula re-rotation and ciliary movements. After confirmation of the ability for neurula re-rotation in mutant Arl13B-expressing *Halocynthia* embryos (gray bar), the embryos were preincubated with Ciliobrevin D. Then, the occurrence of the next re-rotation (A) and ciliary movements (B) were monitored. Control embryos were treated with DMSO. (C) Serial snapshots of cilia in embryos treated with DMSO and Ciliobrevin D. The same cells are traced and indicated by colored circles. Snapshots are aligned at 3 s intervals. Cilia in the Ciliobrevin D–treated embryos look like dots because they stood vertically. See also Supplementary Movie S4. (D) Suppression of neurula rotation in *Ciona* before and after treatment with Ciliobrevin D.

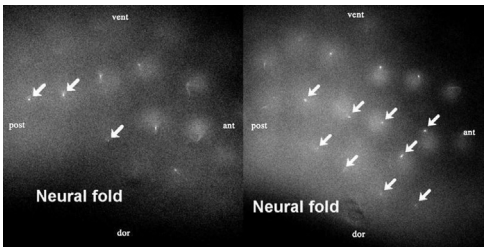

Movie S5. Ciliary movements at the end of re-rotation. Arrows indicate non-motile cilia of epidermal cells close to the neural fold. Time-lapse recording was carried out with intervals of 1 s. The movie runs at 10 frames/s, so it plays 10 times faster than real time.Supplementary material related to this article can be found online at doi:10.1016/j.ydbio.2018.07.023.

cells close to the neural fold looked like dots as they stood up vertically and did not move (Fig. 7, arrows). This is probably because epidermal cells close to the neural fold do not have contact with the vitelline membrane. There are dents on both sides of the neural fold that consist of the transition of the curvature from epidermis to the protruding neural fold (see Fig. 1A). Therefore, cilia without contact with the vitelline membrane do not move. It is likely that rotation stops for two reasons: the physical obstacle of the neural fold and the embryonic surface with cilia close to the neural fold detaching from the vitelline membrane.

Initiation of re-rotation was also observed (Supplementary Movie S6). Embryos immediately started re-rotation, and the speed was gradually accelerated. Most cilia moved and were oriented in the proper direction from the beginning.

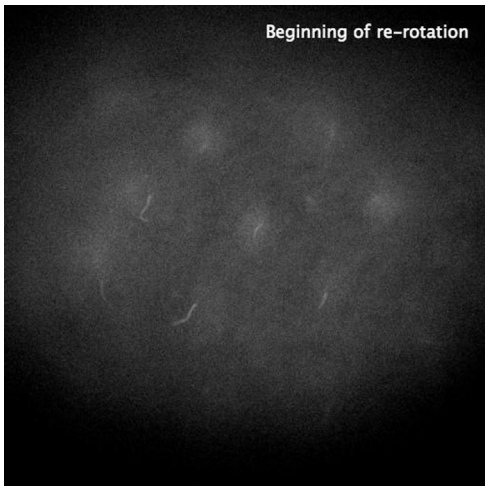

Movie S6. Ciliary movements at the initiation of re-rotation. Time-lapse recording was carried out with intervals of 1 s. The movie runs at 10 frames/s, so it plays 10 times faster than real time.Supplementary material related to this article can be found online at doi:10.1016/j.ydbio.2018.07.023.

We wondered how most of the cilia pointed in the proper direction for the stereotyped counter-clockwise rotation. So we attempted to monitor the initial processes of neurula rotation (not re-rotation) and cilia formation. As already mentioned, it was difficult to record neurula rotation because it lasts only 10 min after 15 h of development and because of the natural developmental asynchrony at this stage. It was

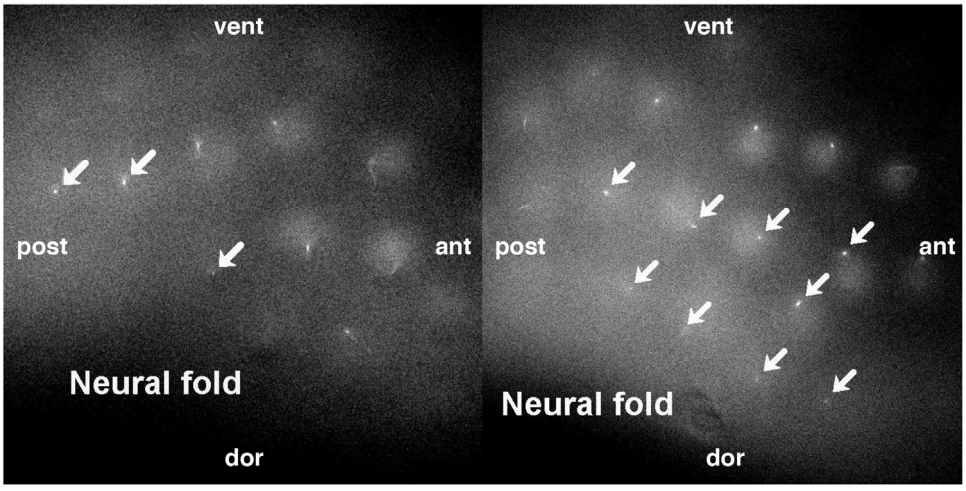

Fig. 7. End of re-rotation. Two examples of the last snapshots at the end of re-rotation movies (Supplementary Movie S5). The neural fold is facing downward. Arrows indicate non-motile cilia of epidermal cells close to the neural fold. They look like dots, as they stood up vertically and did not move. ant, anterior. post, posterior. dor, dorsal. vent, ventral.

Table 1
Differences in neurula rotation between *Halocynthia* and *Ciona*.

	Halocynthia roretzi	***Ciona robusta***
Egg diameter	280 μm	130 μm
Perivitelline space	wide	narrow
Test cells	Aggregated into several cell masses and devoid from the bottom of embryos	Scattered in the entire perivitelline space
Stage	Neurula: 15 h after fertilization at 13 °C	Neurula-initial tailbud: 7.3–8.3 h at 19 °C
Duration	10 min	60 min
Velocity	10°/min	7°/min
Total angle	Less than 360°	Greater than 360° (450° on average, n = 194)
Orientation at the end	Left side down	Various orientations (anterior down, 9%; posterior, 9%; dorsal, 30%; ventral, 7%; left 23%; right 23%; n = 200)
Nodal expression	Left-side epidermis	Left-side epidermis
Mechanism for *nodal* induction	Contact of left-side epidermis with the vitelline membrane	Unknown (devitellinated embryos express *nodal* on both sides).

Movie S7. Cilia formation and their movement at the initiation of rotation. Time-lapse recording was carried out with intervals of 5 s. The movie runs at 10 frames/s, so it plays 50 times faster than real time.Supplementary material related to this article can be found online at doi:10.1016/j.ydbio.2018.07.023.

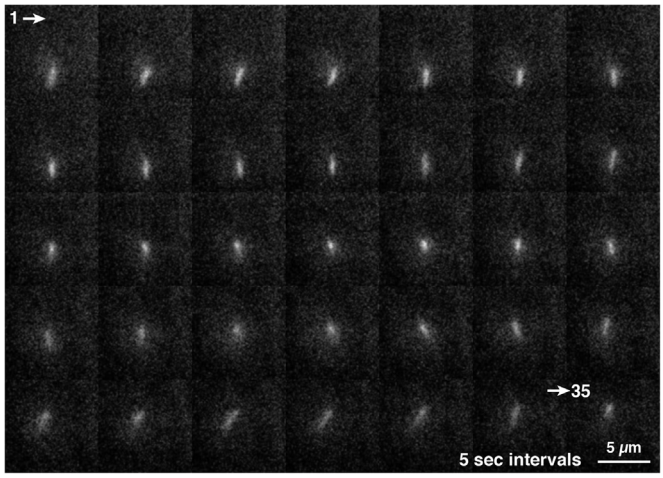

Fig. 8. Ciliary movements in *Ciona*. Cilia were visualized using mutant *Halocynthia* Arl13b fusion protein. A single cilium shown in Supplementary Movie S9 was followed using the "StackReg" function of Image J. Snapshots are aligned at 5 s intervals.

also difficult to focus beforehand on the surface of epidermal cells where cilia will form. The movie images were recorded every 5 s this time, but not 1 s, to allow longer-term recording. Finally, we succeeded in recording rotation just once (Supplementary Movie S7). In the beginning, short cilia appeared. The embryo fluctuated and then rotated in the wrong direction (this does not always happen in neurula rotation). Eventually, it suddenly began rotation in the proper direction. The time resolution of the movie was not high enough to resolve how cilia were formed and oriented in the proper direction for rotation.

3.5. Ciliary movements in Ciona robusta

There are some differences in the features of neurula rotation between *Halocynthia* and *Ciona* (Nishide et al., 2012). We recorded (Supplementary Movie S8) and measured the properties of rotation in *Ciona*, and they are summarized in Table 1. Rotation lasted 60 min, and embryos rotated more than 360°. They did not cease rotation when the left side faced the bottom.

It has been proposed that cilia are non-motile in *Ciona* because the axoneme organization is disorganized, per ultrastructural observation (Thompson et al., 2012). Therefore, we monitored cilia movements in *C. robusta* with *Halocynthia* mutant Arl13b fusion protein. The cilia were indeed moving (Fig. 8, Supplementary Movie S9) in a similar way to those in *Halocynthia*. We observed such movements in three independent observations. The cilia length was short (2.4 μm, n = 12). Cilia shook their tips in the opposite direction of rotation, but cilia were rather linear and a wavy shape of cilia was not observed, probably because of their short length. In addition, the plane of the shaking was not completely flat, unlike that in *Halocynthia*. Our movie was compressed from a Z-stack of five focus planes each 0.55 μm apart. Nevertheless, the movement of some cilia was still out of focus. *Ciona* embryos are entirely surrounded by test cells within the narrow perivitelline space. Therefore, cilia would move on the bumpy surface of the test cell carpet. This coincides with the observation that brief hypo-osmotic shock results in the destruction of test cells and prevents neurula rotation, probably from losing the foothold for cilia to generate a counter-force in *Ciona* (Katsumoto et al., 2013).

To provide further evidence, treatment with dynein inhibitor was also carried out. In the case of *Ciona*, neurula rotation lasted for an hour. Embryos were time-lapse recorded for 15 min to confirm that rotation had started. Then the same embryos were treated with Ciliobrevin D for 15 min. After the treatment, rotation was recorded again for 30 min. A total of 94% of embryos rotated before the treatment, but none of them showed rotation after the treatment (Fig. 6D). Therefore, ciliary movements also drive neurula rotation in *Ciona*.

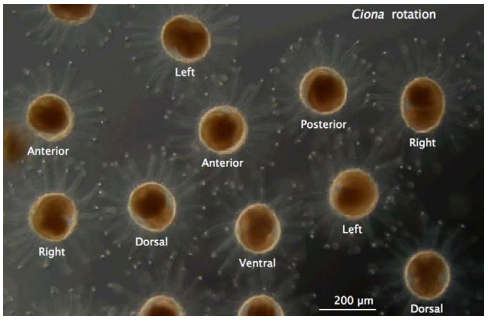

Movie S8. Neurula rotation of *Ciona robusta*. At the end of the movie, the sides of embryos that are oriented downwards are shown. Time-lapse recording was carried out with intervals of 60 s. The movie runs at 30 frames/s, so it plays 1800 times faster than real time. The movie shows a sequence of approximately 1 h.Supplementary material related to this article can be found online at doi:10.1016/j.ydbio.2018.07.023.

4. Discussion

The present results suggest that slow and serpentine movement of epidermis monocilia drive ascidian neurula rotation in both *Halocynthia* and *Ciona*. This is supported by the following observa-

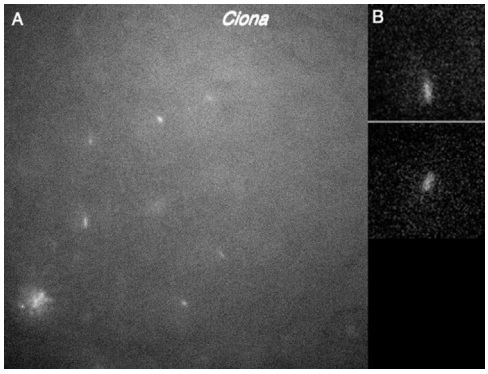

Movie S9. Ciliary movements in *Ciona* neurula rotation. Time-lapse recording was carried out with intervals of 5 s. The movie runs at 10 frames/s, so it plays 50 times faster than real time. The movie was compressed from a Z-stack of five focus planes each 5.5 μm apart using "Sum slices" in the Z projection function of Image J. (A) Neurula embryo observed from the bottom. (B) Two examples of cilia were followed using the "StackReg" function of Image J.Supplementary material related to this article can be found online at doi:10.1016/j.ydbio.2018.07.023.

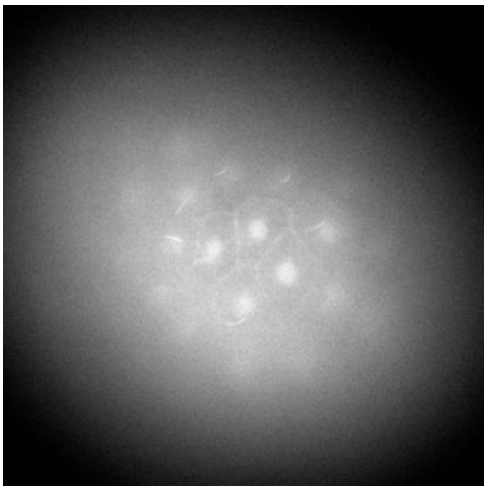

Movie S10. Movements of cilia on an embryo that showed abnormal rotation. The embryo changed its direction of rotation several times. It seems that most cilia are swept towards the opposite direction of rotation when it changed direction of the rotation. Time-lapse recording was carried out with intervals of 5 s. The movie runs at 5 frames/s, so it plays 25 times faster than real time.Supplementary material related to this article can be found online at doi:10.1016/j.ydbio.2018.07.023.

tions. There is a good correlation between when cilia are present and the capacity for re-rotation (Nishide et al., 2012). The longer the cilia were, the faster was the rotation. Cilia were pointed in the opposite direction of rotation to generate the counter-force. When mutant Arl13b was overexpressed, it inhibited both rotation and ciliary movement. Treatment with dynein inhibitor prevented ciliary movement, and the rotation of embryos was abrogated. When the dynein inhibitor treatment was initiated before neurula rotation, the formation of cilia was impaired and embryos did not rotate.

Our observations suggest that embryos rotate by generating a counter-force with cilia that crawl on the inner surface of the vitelline membrane as a substrate or foothold but not by generating a water current around embryos. Previously, fluorescent microbeads (FluoSpheres) injected into the perivitelline space showed no indication of a water current around the embryos (Nishide and Nishida, unpublished observation). Denuded embryos could not rotate on the agar plate. When the bottom of the vitelline membrane was flattened by attachment to glass or by compression onto glass, they did not rotate. This indicates that the curvature of the vitelline membrane is important and that a certain amount of contact between the membrane and embryonic surface is essential to generate enough force. Finally, only cilia that have contact with the vitelline membrane were motile. Those on the top of the embryos and in dents on both sides of the neural fold were standing vertically and did not move. All of these support the conclusion that cilia that crawl on inner surface of the vitelline membrane generate the counter-force for rotation.

The movement of the epidermal cilia showed some unique characteristics. They moved very slowly, at one cycle per 7.6 s. They moved in a serpentine way like flagella and lie in a narrow space between embryos and the vitelline membrane or test cells. To our knowledge, there is no other example that the monocilia of multicellular epithelium show such a wavy movement. In addition, it seems that only cilia that have contact with the vitelline membrane and lie on the cell surface are motile. In these respects, ascidian epidermis cilia are very unique.

It is possible that ascidian cilia are rotating cilia by nature. But their movement is squashed and confined to a flat plane, as it is restricted in a narrow space between the embryo and the vitelline membrane. The movement of rotating cilia in the mouse node, with a relatively shorter and more linear shape (Okada et al., 2005), resembles that of *Ciona* cilia when squashed into a planar space and that of rotating cilia in the gastrocoel roof plate of *Xenopus* and Kupffer's vesicle of zebrafish (Schweickert et al., 2007; Kramer-Zucker et al., 2005; Lu et al., 2015) with a longer and spiral shape looks like that of *Halocynthia* cilia. By chance, we recorded movements of cilia on an embryo that showed abnormal rotation (Supplementary Movie S10). The embryo opportunistically changed its direction of rotation several times. It appeared that most cilia were pushed and redirected when the embryo changed its direction of rotation. Although this is an observation of anomalistic rotation, it is implied that ascidian cilia are able to move in any direction. This is consistent with the hypothesis that ascidian cilia are rotating by nature. If this is the case, ascidian epidermis cilia are more similar to the rotating cilia of the vertebrate L-R organizers, although ascidian embryos rotate as a whole similarly to embryos of non-vertebrate deuterostomes, such as echinoderm, hemichordate, and amphioxus, while swimming. Recently it was reported that sea urchin embryos also utilize cilia to break the L-R symmetry (Su, 2014; Takemoto et al., 2016; Tisler et al., 2016), although there is disagreement on where are relevant cilia among these reports.

In mouse, cilia in the node shift posteriorly on each cell and they tilt posteriorly in order to generate leftward nodal flow (Okada et al., 2005). The bases of cilia showed no positional bias in *Halocynthia* (Nishide et al., 2012 and the present study). In contrast, those in *Ciona* have a strong bias toward the posterior side of each epidermal cell (Thompson et al., 2012; Negishi et al., 2016; Palmquist and Davidson, 2017). It is unclear whether the posterior bias plays an essential role for neurula rotation as the orientation of motile cilia of *Ciona* is perpendicular to the anteroposterior axis, as well as in *Halocynthia*.

It is still unclear how the direction of ciliary movement is regulated. There should be a certain polarity in the epidermal cell sheet. The polarity is perpendicular to the anteroposterior axis and runs through the transverse surface of embryos. Once rotation has started, it could be possible that every cilium is swept by the shearing force of rotation movement at the contact site with the vitelline membrane, and then they begin to move in the same direction since cilia without contact with the vitelline membrane just stand up vertically. We also received this impression from the coordinated ciliary movements shown in Supplementary Movie S10. Therefore, the orientation of most cilia is passively coordinated in the same direction by the embryonic rotation itself. But we still do not know how the orientation of emerging cilia is biased in the correct direction at the beginning of the initial rotation and why all of the cilia are oriented in the proper direction at the beginning of re-rotation before re-rotation starts.

The planar cell polarity (PCP) pathway would be hypothesized to regulate the polarity of the epidermal cell sheet. Echinoderm, hemichordate, and amphioxus embryos have chirality in their epidermis since they swim while rotating in the same direction as the ascidian neurula rotation (Satoh, 2009). It has been shown that the PCP in ectoderm orients cilia for swimming during cnidarian larval development (Momose et al., 2012), and it is also involved in the orientation of node cilia in mouse (Minegishi et al., 2017). Therefore, ascidians transform the chirality of the embryonic epidermis sheet in reference to the anteroposterior axis into L-R asymmetry, while vertebrates break symmetry by utilizing the chirality of cilia rotation based on the cilia ultrastructure in reference to the anteroposterior axis.

Acknowledgments

We thank the members of the Asamushi Research Center for Marine Biology and the Onagawa Field Center for help in collecting live ascidian adults, and the Seto Marine Biological Laboratory for help in maintaining them. This work was supported by Grants-in-Aid from the Japan Society for the Promotion of Science (22370078, 15H04377), and from the Ministry of Education, Culture, Sports, Science and Technology, Japan (25113518) to H.N. *Ciona robusta* adults were supplied by the National Bio Resource Project (NBRP, Japan).

Author contributions

H.N. conceived and directed this study. S.Y. and Y.T. carried out the primary parts of the experiments. K.S.I. and T.A.O. contributed to plasmid construction, and K.S.I to *Ciona* microinjection. M.S. measured the properties of *Ciona* rotation. S.Y., Y.T. and H.N. wrote the manuscript.

Appendix A. Supporting information

Supplementary data associated with this article can be found in the online version at doi:10.1016/j.ydbio.2018.07.023.

References

Akanuma, T., Hori, S., Darras, S., Nishida, H., 2002. Notch signaling is involved in neurogenesis in the ascidian embryos. Dev. Genes Evol. 212, 459–472.

Blum, M., Feistel, K., Thumberger, T., Schweickert, A., 2014. The evolution and conservation of left-right patterning mechanisms. Development 141, 1603–1613.

Brozovic, M., Dantec, C., Dardaillon, J., Dauga, D., Faure, E., Gineste, M., Louis, A., Naville, M., Nitta, K.R., Piette, J., Reeves, W., Scornavacca, C., Simion, P., Vincentelli, R., Bellec, M., Aicha, S.B., Fagotto, M., Gueroult-Bellone, M., Haeussler, M., Jacox, E., Lowe, E.K., Mendez, M., Roberge, A., Stolfi, A., Yokomori, R., Brown, T., Cambillau, C., Christiaen, L., Delsuc, F., Douzery, E., Dumollard, R., Kusakabe, T., Nakai, K., Nishida, H., Satou, Y., Swalla, B., Veeman, M., Volff, J-N., Lemaire, P., 2018. ANISEED 2017: Extending the integrated ascidian database to the exploration and evolutionary comparison of genome-scale datasets. Nucleic Acids Res. 46, D718–D725.

Cevik, S., Hori, Y., Kaplan, O.I., Kida, K., Toivenon, T., Foley-Fisher, C., Cottell, D., Katada, T., Kontani, K., Blacque, O.E., 2010. Joubert syndrome Arl13b functions at ciliary membranes and stabilizes protein transport in *Caenorhabditis elegans*. J. Cell Biol. 188, 953–969.

Firestone, A.J., Weinger, J.S., Maldonado, M., Barlan, K., Langston, L.D., O'Donnell, M., Gelfand, V.I., Kapoor, T.M., Chen, J.K., 2012. Small-molecule inhibitors of the AAA+ ATPase motor cytoplasmic dynein. Nature 484, 125–129.

Geng, L., Okuhara, D., Yu, Z., Tian, X., Cai, Y., Shibazaki, S., Somlo, S., 2006. Polycystin-2 traffics to cilia independently of polycystin-1 by using an N-terminal RVxP motif. J. Cell Sci. 119, 1383–1395.

Hori, Y., Kobayashi, T., Kikko, Y., Kontani, K., Katada, T., 2008. Domain architecture of the atypical Arf-family GTPase Arl13b involved in cilia formation. Biochem. Biophys. Res. Commun. 373, 119–124.

Katsumoto, S., Hatta, K., Nakagawa, M., 2013. Brief hypo-osmotic shock causes test cell death, prevents neurula rotation, and disrupts left-right asymmetry in *Ciona intestinalis*. Zool. Sci. 30, 352–359.

Kramer-Zucker, A.G., Olale, F., Haycraft, C.J., Yoder, B.K., Schier, A.F., Drummond, I.A., 2005. Cilia-driven fluid flow in the zebrafish pronephros, brain and Kupffer's vesicle is required for normal organogenesis. Development 132, 1907–1921.

Kumano, G., Yamaguchi, S., Nishida, H., 2006. Overlapping expression of FoxA and Zic confers responsiveness to FGF signaling to specify notochord in ascidian embryos. Dev. Biol. 300, 770–784.

Lu, H., Toh, M.T., Narasimhan, V., Thamilselvam, S.K., Choksi, S.P., Roy, S., 2015. A function for the Joubert syndrome protein Arl13b in ciliary membrane extension and ciliary length regulation. Dev. Biol. 397, 225–236.

Makabe, K.W., Kawashima, T., Kawashima, S., Minokawa, T., Adachi, A., Kawamura, H., Ishikawa, H., Yasuda, R., Yamamoto, H., Kondoh, K., Arioka, S., Sasakura, Y., Kobayashi, A., Yagi, K., Shojima, K., Kondoh, Y., Kido, S., Tsujinami, M., Nishimura, N., Takahashi, M., Nakamura, T., Kanehisa, M., Ogasawara, M., Nishikata, T., Nishida, H., 2001. Large-scale cDNA analysis of the maternal genetic information in the egg of the ascidian, *Halocynthia roretzi*, for the gene expression catalog during development. Development 128, 2555–2567.

Minegishi, K., Hashimoto, M., Ajima, R., Takaoka, K., Shinohara, K., Ikawa, Y., Nishimura, H., McMahon, A.P., Willert, K., Okada, Y., Sasaki, H., Shi, D., Fujimori, T., Ohtsuka, T., Igarashi, Y., Yamaguchi, T.P., Shimono, A., Shiratori, H., Hamada, H., 2017. A Wnt5 activity asymmetry and intercellular signaling via PCP proteins polarize node cells for left-right symmetry breaking. Dev. Cell. 40, 439–452.

Momose, T., Kraus, Y., Houliston, E., 2012. A conserved function for Strabismus in establishing planar cell polarity in the ciliated ectoderm during cnidarian larval development. Development 139, 4374–4382.

Morokuma, J., Ueno, M., Kawanishi, H., Saiga, H., Nishida, H., 2002. *HrNodal*, the ascidian *nodal*-related gene, is expressed in the left side of the epidermis, and lies upstream of *HrPitx*. Dev. Genes Evol. 212, 439–446.

Namigai, E.K., Kenny, N.J., Shimeld, S.M., 2014. Right across the tree of life: the evolution of left-right asymmetry in the Bilateria. Genesis 52, 458–470.

Negishi, T., Miyazaki, N., Murata, K., Yasuo, H., Ueno, N., 2016. Physical association between a novel plasma-membrane structure and centrosome orients cell division. eLife 5, e16550.

Nishide, K., Mugitani, M., Kumano, G., Nishida, H., 2012. Neurula rotation determines left-right asymmetry in ascidian tadpole larvae. Development 139, 1467–1475.

Nonaka, S., Tanaka, Y., Okada, Y., Takeda, S., Harada, A., Kanai, Y., Kido, M., Hirokawa, N., 1998. Randomization of left-right asymmetry due to loss of nodal cilia generating leftward flow of extraembryonic fluid in mice lacking KIF3B motor protein. Cell 95, 829–837.

Nonaka, S., Shiratori, H., Saijoh, Y., Hamada, H., 2002. Determination of left-right patterning of the mouse embryo by artificial nodal flow. Nature 418, 96–99.

Okada, Y., Takeda, S., Tanaka, Y., I-Belmonte, J.C., Hirokawa, N., 2005. Mechanism of nodal flow: a conserved symmetry breaking event in left-right axis determination. Cell 121, 633–644.

Palmquist, K., Davidson, B., 2017. Establishment of lateral organ asymmetries in the invertebrate chordate, *Ciona intestinalis*. EvoDevo 8, 12.

Satoh, N., 2009. An advanced filter-feeder hypothesis for urohordate evolution. Zool. Sci. 26, 97–111.

Schweickert, A., Weber, T., Beyer, T., Vick, P., Bogusch, S., Feistel, K., Blum, M., 2007. Cilia-driven leftward flow determines laterality in *Xenopus*. Curr. Biol. 17, 60–66.

Spéder, P., Petzoldt, A., Suzanne, M., Noselli, S., 2007. strategies to establish left/right asymmetry in vertebrates and invertebrates. Curr. Opin. Genet. Dev. 17, 351–358.

Su, Y.H., 2014. Telling left from right: left-right asymmetric controls in sea urchins. Genesis 52, 269–278.

Takaoka, K., Yamamoto, M., Hamada, H., 2007. Origin of body axes in the mouse embryo. Curr. Opin. Genet. Dev. 17, 344–350.

Takemoto, A., Miyamoto, T., Simono, F., Kurogi, N., Shirae-Kurabayashi, M., Awazu, A., Suzuki, K.T., Yamamoto, T., Sakamoto, N., 2016. Cilia play a role in breaking left-right symmetry of the sea urchin embryo. Genes Cells 21, 568–578.

Taniguchi, K., Nishida, H., 2004. Tracing cell fate in brain formation during embryogenesis of the ascidian *Halocynthia roretzi*. Dev. Growth Differ. 46, 163–180.

Thompson, H., Shaw, M.K., Dawe, H.R., Shimeld, S.M., 2012. The formation and positioning of cilia in *Ciona intestinalis* embryos in relation to the generation and evolution of chordate left-right asymmetry. Dev. Biol. 364, 214–223.

Tisler, M., Wetzel, F., Mantino, S., Kremnyov, S., Thumberger, T., Schweickert, A., Blum, M., Vick, P., 2016. Cilia are required for asymmetric nodal induction in the sea urchin embryo. BMC Dev. Biol. 23, 28.

Vandenberg, L.N., Levin, M., 2013. A unified model for left-right asymmetry? Comparison and synthesis of molecular models of embryonic laterality. Dev. Biol. 379, 1–15.

Yoshida, K., Saiga, H., 2008. Left-right asymmetric expression of *Pitx* is regulated by the asymmetric *Nodal* signaling through an intronic enhancer in *Ciona intestinalis*. Dev. Genes Evol. 218, 353–360.

Yoshida, K., Saiga, H., 2011. Repression of Rx gene on the left side of the sensory vesicle by *Nodal* signaling is crucial for right-sided formation of the ocellus photoreceptor in the development of *Ciona intestinalis*. Dev. Biol. 354, 144–150.